ON VASCULAR BUNDLE MODIFICATIONS IN NODES AND INTERNODES OF SELECTED GRASS SPECIES

H. Kraehmer

Kantstrasse 20, D-65719 Hofheim, Germany

Grass nodes play an essential role as interfaces between leaf and stem. The description of the bundle course in nodes considerably contributes to understanding of the transport of assimilates, minerals, and xenobiotics in grasses. Nodes and internodes of 38 species of the subfamilies Arundinoideae, Bambusoideae, Panicoideae, and Pooideae were analyzed histologically. Free-hand sections, various staining techniques, macro- and microphotography were used to reveal a few principles underlying their anatomy. In all grass species, specific nodal zones were found in which many vascular bundles undergo characteristic transformations. This transformation starts with the augmentation of xylem in lower nodal areas and continues with the formation of specific amphivasal structures providing connections with the leaf attached to the node. The anatomy of these strands, herein called vasotubuli, has not much in common with vascular bundles in internodes any more. Transverse nodal plexus strands provide many connections between bundles and vasotubuli. The nodal plexus is also an interface of sclerenchyma bundles. The nodes of most grass species are constructed very similarly with a few exceptions: the nodes of *Phragmites australis* (Cav.) Steud. for example have something in common with bamboo: they develop spindle-like glomeruli.

Poaceae, phloem, xylem, glomeruli, nodal plexus, anatomy

DE GRUYTER OPEN

doi: 10.1515/sab-2017-0018
Received for publication on January 27, 2016
Accepted for publication on March 22, 2017

INTRODUCTION

Grasses are built from similarly constructed modules, so called phytomers (Esau, 1943). This phenomenon has recently been discussed by Fournier, Andrieu (2000) for maize and Forster et al. (2007) for barley. Culms consist of nodes and internodes. Nodes have their origin in meristematic zones of early grass development. Leaves, buds, and sometimes shoot-borne roots are inserted at nodes. Leaves inserting at nodes surround the stem and form a leaf sheath. Leaf, leaf sheath, internode, node, and bud together form a phytomer. Arber (1934) already explained the vasculature in Gramineae systematically. Kumazawa (1942, 1946, 1961), Sharman (1942), and Esau (1943) were among the first scientists to analyze the course of vascular bundles in maize internodes and nodes in a detailed way. Hitch, Sharman (1971) as well as Zimmerman, Tomlinson (1972) tried to elucidate the arrangements of vascular bundles within stems of monocots by diagrammatic representations. The course of bundles has been investigated in different monocot species in the past, especially in context with primary and secondary thickening processes as for example in palm trees, onion, *Yucca* species or *Cordyline terminalis* (e.g. DeMason, 1994). Zimmermann, Tomlinson (1972) based their findings primarily on palm trees and on species that unfortunately also do not belong to the Poaceae family. Grass specific studies were rather rare in the last decades with a few exceptions.

Bell, Wynn Parry (1976) and Bell (1976a, b) produced three-dimensional sketches of *Lolium multiflorum* Lam. nodes. In the 80s of the last century, a major approach towards the explanation of wheat nodes was published by Patrick (1972a, b).

Lersten (1987) compiled an overview on the anatomy of wheat with some new views on nodes. Hoshikawa (1989) published details on the structure of rice nodes. Pizzolato (2000) provided a more systematic approach in comparing different grass species.

All reconstructions of bundle courses in literature are primarily based on sketches derived from sequential pictures. The actual course of bundles was demonstrated in very few plants only such as in macerated maize plants by Sharman (1942).

Most botanists just use the term vascular bundle for all conduits running through nodes. Some grass bundles, however, are completely changed or modified within nodes as will be shown here, they form strands of different morphological appearance, they branch or they merge with other bundles and cannot be traced back easily to their origins.

The area, in which transverse bundles are found within nodes, is called nodal plexus (Hitch, Sharman, 1971). Shane et al. (2000) studied the vascular system in maize and used their results to discuss the high redundancy of bundle connections within the nodal plexus.

Nodal plexus structures seem to be rather characteristic of the Poaceae family. At least Tomlinson (1995) refers to monocotyledons without a nodal plexus.

Ayensu (1972) summarizes results on a phenomenon that was originally regarded as specific for the Dioscoreaceae family – so-called glomeruli in nodes. These are defined as very complex and peculiar assemblages of vascular cells. In the 90s of the last century, Liese (1998) found similar glomeruli in the nodes of bamboo. Until now, other findings of glomeruli have not been published.

The arrangement of vascular bundles in internodes of grasses can vary to some extent. Fahn (1990) distinguishes between two types of Gramineae stems: one in which vascular bundles are arranged in two circles and one in which vascular bundles are scattered throughout the entire cross-section of the stem. Differences in bundle patterns of various grass species were highlighted by earlier botanists (e.g. by Stover, 1934). In consequence, one can expect to see differences in the anatomy of nodes, too. Patrick (1972a, b) tried to identify for wheat how medians, laterals, and intermediates of leaves correspond with bundles in internodes. His explanations for the origin of sclerenchyma bundles is, however, not completely satisfying.

Nodes play an essential role as interfaces between leaf and stem in higher plant species. They are vital parts of the elements transporting water and assimilates within plants. Yamaji, Ma (2009) reported that the expression of an influx transporter of silicon is especially increased in node 1 of rice (the one below the panicle). Xylem transfer cells in nodes seem to play a special role in this context. The same authors list a number of mineral transporters specific of nodes in rice (Yamaji, Ma, 2014). Unfortunately, the three-dimensional structure of grass nodes is quite complicated. The objective of this paper is therefore to show that a systematic analysis and zonation of vascular bundle modifications in nodes of different grass species can help understand how grass nodes are structured in principal. Another aspect is the detection of so far undescribed specific nodal structures.

MATERIAL AND METHODS

Plant material

Most plant parts analyzed were collected from outdoor plants found near Frankfurt, Germany. Some grass species were bought as ornamentals from garden centres or grown from seeds in pots under glasshouse conditions. Tables 1, 2 show the investigated species and the number of analyzed plants.

Histology

At least three nodes of each species were analyzed. Too thin longitudinal sections of grass culms are not suitable to demonstrate the course of bundles directly as bundles often change directions slightly within the stem. This is why thick sections and special staining procedures were used here. Nodes and internodes were sequentially cut in transverse and longitudinal sections with razor blades by hand. The sections were stained as described by Kraehmer, Baur (2013). Totally 40–50 transverse sections were prepared per node. Thick sections (between 10 and 200 µm) were stained on glass slides in different staining procedures: (a) with 0.1–1% toluidine blue in water solutions; (b) with a modified Etzold Blue or FCA mixture (fuchsin, chrysoidine, astra blue) published by Henkel (2003). Sections were pre-stained in a droplet of an astra blue solution (2 g in 100 ml water and 2 ml glacial acetic acid) on the microscope slide for a few seconds. Then, a droplet of the FCA solution was added. The sections were finally rinsed with water on the microscope slide as described by Kraehmer, Baur (2013); (c) with a modified version of Wacker's (2006) trichromatic W-3A botanical staining procedure involving astra blue, acridine red, and acriflavine (acridine red solution: 1 g acridine red 3B in 100 ml 50% ethanol with 2 ml glacial acetic acid; acriflavine solution: 1 g acriflavine in 100 ml water plus 2 ml glacial acetic acid). Similarly to the method described in (b), the sections were pre-stained with a droplet of the astra blue solution for a few seconds, then a droplet of the acridine red solution was added and thereafter a small droplet of the acriflavine solution. This sequence is important to get the same staining results. Finally, the sections were rinsed with water on the microscope slide.

Table 1. Analysis of grass group A – number of plants (*n*), month of analysis, and bundle patterns in fully developed internodes

Subfamily	Species	*n*	Month_Year (20xx)	Pattern
Arundinoideae	*Arundo donax* L.	8	11_14; 08 to 11_15	S
	Hakonechloa macra (*Munro*) *Honda*	3	8_15; 3_16; 7_16	R
	Molinia caerulea (L.) Moench	4	10_14; 8_15; 7_16	R
	Phragmites australis (Cav.) Steud.	12	7_14; 9_14; 8_15; 7_16	I
Bambusoideae	*Fargesia murielae* Gamble	2	10_16	S
	Indocalamus latifolius (Keng) McClure	1	10_16	S
	Phyllostachys aurea Rivière & C.Rivière	4	12_16	S
Panicoideae	*Arthraxon ciliaris* P.Beauv.	1	9_16	R
	Cymbopogon citratus (DC.) Stapf	3	10_16	S
	Digitaria sanguinalis (L.) Scop.	3	9_15	R
	Echinochloa crus-galli (L.) P.Beauv.	8	7 + 8_14	I
	Imperata cylindrica (L.) Raeusch.	3	10_16	S
	Miscanthus x giganteus J.M.Greef, Deuter ex Hodk., Renvoize	3	11_16	S
	Pennisetum alopecuroides (L.) Spreng.	2	10_15	I
	Setaria glauca (L.) P.Beauv.	4	8_14	R
	Sorghum halepense (L.) Pers.	8	8_14; 10 + 11_15	S
	Zea mays L.	3	7 + 8_14	S

S = scattered over section, R = 2–3 ring-like arrangements, I = Intermediate

Table 2. Analysis of grass group B (Pooideae) – number of plants (*n*), month of analysis, and bundle patterns in fully developed internodes

Species	*n*	Month_Year (20xx)	Pattern
Achnatherum calamagrostis (L.) P.Beauv.	3	8_15	R
Alopecurus geniculatus L.	2	1_16	R
Alopecurus myosuroides Huds.	3	5_15	R
Alopecurus pratensis L.	3	5_15	R
Apera spica-venti (L.) P.Beauv.	1	6_16	R
Arrhenaterum elatius (L.) P.Beauv. ex J.Presl & C.Presl	5	6_14; 4 + 5_15	R
Avena fatua L.	6	7_14; 6_15	R
Avena sativa L.	11	10_14; 11 + 12_15; 1_16	R
Brachypodium sylvaticum (Huds.) P.Beauv.	2	9_15	R
Bromus tectorum L.	6	4 + 5_15; 5_16	R
Dactylis glomerata L.	7	10_14; 4 + 5 + 12_15; 2_16	R
Festuca gigantea (L.) Vill.	3	8 + 10_14	R
Glyceria maxima (Hartm.) Holmb.	3	4_13; 6 + 7_14	R
Hordeum vulgare L.	6	3_15; 1 + 3 + 4_16	R
Lolium multiflorum Lam.	3	3_15;7_16	R
Milium effusum L.	4	5_15; 5_16	R
Phalaris arundinacea L.	8	4–6_15	R
Poa bulbosa L.	1	4_16	R
Poa pratensis L.	1	4_16	R
Secale cereale L.	4	3–6_16	R
Triticum aestivum L.	8	12_14; 5 + 6_15; 1–6_16	R

R = 2–3 ring-like arrangements

Table 3. Numbers of outer sclerenchyma bundles, of central bundles in internodes and leaf sheaths of *P. australis* (lateral shoot of an outdoor plant; August 24, 2015, stem diameter around 3 mm at internode 6)

Internode[1]	Total	Central bundles	Outer sclerenchyma bundles	Sheath bundles[2]
1	88	38	50	38
2	88	34	54	40
3	101	39	62	38
4	102	36	66	41
5	113	36	77	40
6	113	43	70	49

[1]counting downwards from the first macroscopically visible node after removal of top leaves

[2]sheath bundles at the base of the internode; these bundles extend into the node and internode below

The nodes were usually cut from the lower internode upwards.

Sclerenchyma bundles and inner bundles of Table 3 were counted separately in the middle of an internode. Bundles entering a leaf were counted in the pulvinus area.

***In vivo* tracing**

The origin of single bundles was traced in order to verify where bundles have their origin and how they fit into the existing set of bundles in a given internode. This was achieved by selective pre-staining of vascular bundles with dyes which are transported acropetally in the xylem such as basic fuchsin, also described as rosaniline by K u m a z a w a (1961). For this purpose, stems were cut in a bucket under water. The lower ends were transferred into glass vessels under water in order to avoid air entering vascular bundles. After removing the cut stems in the glass vessels from the bucket, concentrated dye solutions were added to the water in the glass vessels. Several hours to three days later, sections of pre-treated tissues could be analyzed. Basic fuchsin will primarily stain lignified tissues. Dyes are often not transported in all vessels beyond the node above the cut end for reasons not explained here. This makes it possible to follow the course of single bundles.

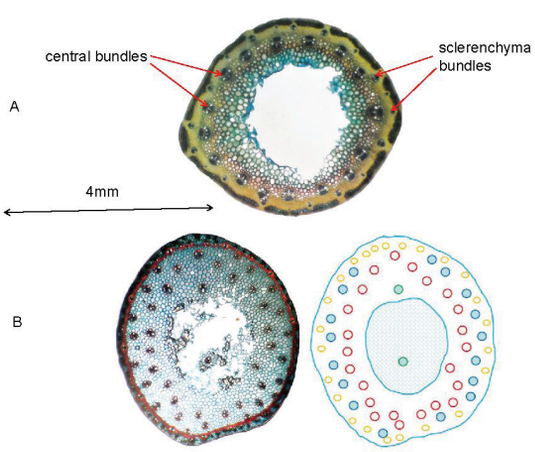

Fig. 1. (A) Two-ring pattern of bundle arrangement in *Poa pratensis*; Wacker staining, ~20×; (B) intermediate pattern of bundles in *Echinochloa crus-galli*; left: Etzold blue staining, ~20×**; right: sketch** with differently stained bundles; yellow: sclerenchyma bundles, blue and red: inner bundle rings, green: two separate bundles in the centre

Documentation

Findings were documented in form of pictures taken with a Nikon D90 camera (Nikon Corp., Japan) mounted on a trinocular Olympus E-microscope (type ECEtr; Olympus Corp., Japan) or on a Bresser Advance ICD stereo microscope with adapters (Bresser GmbH, Germany). Most pictures were processed using Photoshop Elements 2.0 software.

RESULTS

Internode patterns of vascular bundles in the studied objects

Tables 1, 2 provide an overview on the patterns of vascular bundles observed in internodes. Obviously, all analyzed species of the subfamily Pooideae follow the ring-like arrangement defined by F a h n (1990). This type is exemplified by a transverse section of the third internode of *Poa pratensis* in Fig. 1, A. Intermediate patterns with several rows of bundles prevailed for example in the species *Phragmites australis*, *Echinochloa crus galli,* and *Pennisetum alopecuroides,* especially in fully developed, older internodes (Fig. 1, B). The bamboos analyzed here, *Arundo donax* and several representatives of the subfamily Panicoideae are characterized by internodes in which bundles are scattered

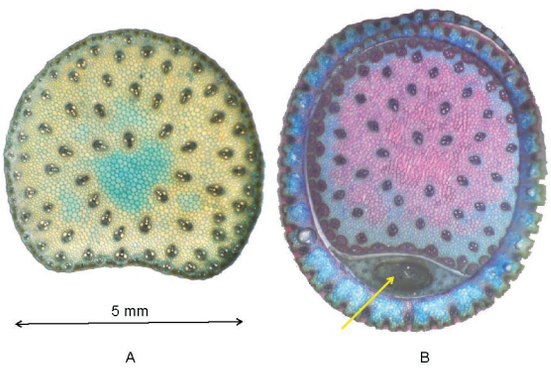

Fig. 2. Internode 1 (A) and internode 2 (B) of *Sorghum halepense*. (A) Wacker staining, (B) Etzold blue staining; ~20×. Internode 2 to the right is surrounded by the leaf sheath with a bud visible at the lower end (yellow arrow)

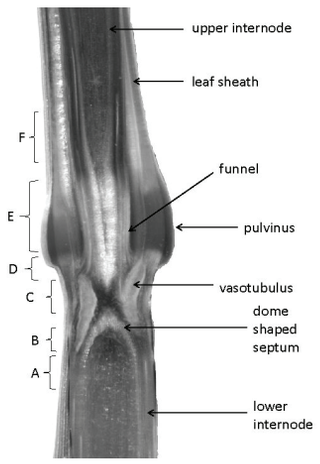

Fig. 3. Macro view of longitudinally cut *Avena fatua* culm at node. A = Lower nodal transition zone (LNTZ), B = Lower vasotubulus zone (LVZ), C = Upper vasotubulus zone (UVZ), D = Leaf insertion zone (LIZ), E = Funnel or pulvinus zone (FZ), F = Internode separation zone (ISZ)

all over the section. Fig. 2 shows the pattern of bundles in node 1 (A) and node 2 (B) of *Sorghum halepense*. Bundle patterns within the same internode stay constant and the relative position of bundles does not change. They change, however, at nodes due to the distich arrangement of leaves. In principle, no bundle pattern is repeated within a culm: the total number of bundles usually increases towards the base of a stem as exemplified by Table 3. Primarily, sclerenchyma bundles are augmented. The number of bundles entering a leaf is always different from that counted in an internode.

Modifications of the vascular system at different levels of pooid, panicoid, and some arundinoid grass nodes

Fig. 3 shows a longitudinal section of a wild oat (*Avena fatua*) node. This type of nodal structure is very common in most pooid grasses. It demonstrates where major changes within nodes can be observed. Structures of nodes in panicoid and arundinoid grasses look sometimes a bit different, especially in species with bundles scattered all over the sections. Many principal modifications such as a characteristic zonation, the modifications of bundles and the formation of nodal

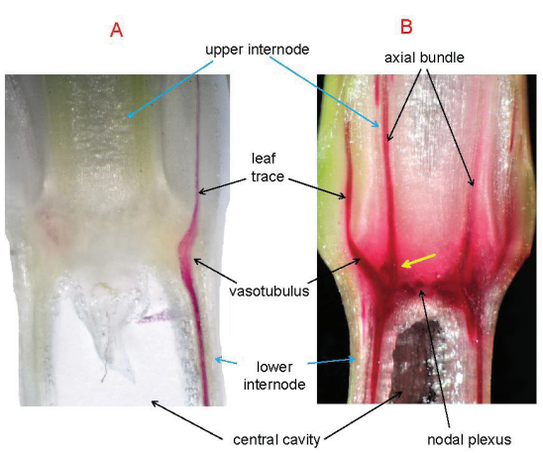

Fig. 4. Bundles course in longitudinally cut *Avena sativa* culm at nodes 1 (A) and 2 (B). The yellow arrow indicates the point where the axial bundle splits and surrounds a vasotubulus; pre-stained with fuchsin, ~20×; culm diameters at base ~4 mm

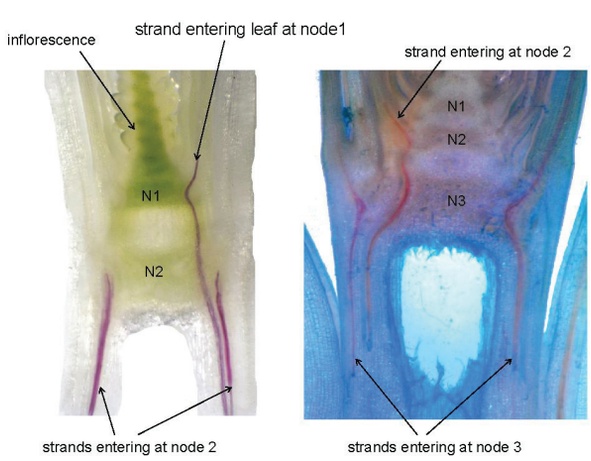

Fig. 5. Longitudinally cut culm of *Triticum aestivum* (left) and *Avena sativa* (right) at tip showing bundle courses and entrance into leaf base. N1–N3 = nodes 1–3. Culm diameters at base 3–4 mm

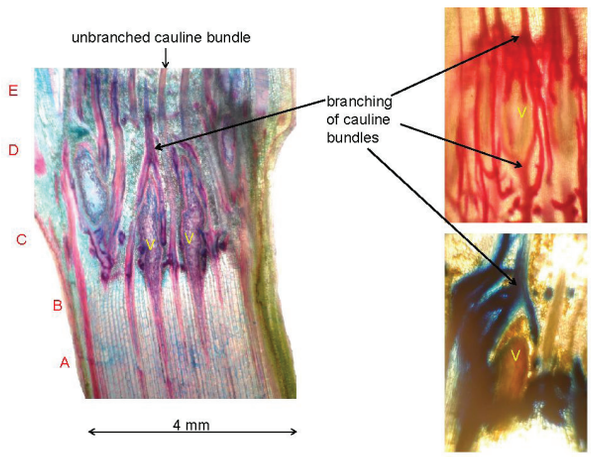

Fig. 6. Longitudinally cut nodes of *Echinochloa crus-galli* (left, Etzold blue), *Dactylis glomerata* (top right, pre-stained with fuchsin, ~40×), and *Avena sativa* (bottom right, methylene blue, ~40×) showing branching and vasotubuli (yellow V) surrounding axial or cauline bundles

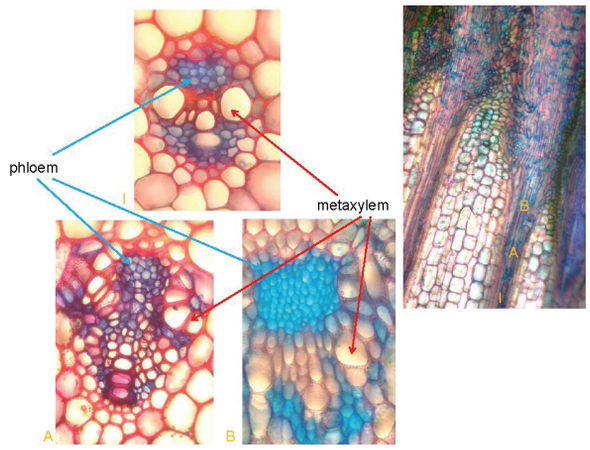

Fig. 7. Transition from internode to node, levels A and B. Top left: *Festuca gigantea* transverse – internode (I), bottom left: Lower nodal transition zone (LNTZ) (A), both Etzold blue, 400×**; bottom right:** *Avena sativa* node transverse, Lower vasotubulus zone (LVZ) (B), Wacker staining, 400×; top right: *Dactylis glomerata*, longitudinal, Etzold blue, 100×

plexus structures are, however, very similar. Details for all species cannot be shown here for the sake of simplicity and clarity. Nodes of *Phragmites australis* are an exception and will be dealt with separately below. As exemplified by Fig. 3, six levels (A–F) can be distinguished in most of the analyzed species.

Many morphological details shown in Fig. 3 are described in classical botany textbooks. Two specific structures not defined in literature so far are therefore highlighted here. The first morphological characteristic is a funnel zone which is usually surrounded by the pulvini at the leaf sheath base. It is located in the lower end area of the internode. The diameter of the internode is usually smaller in this zone than above or in the internode below. A second specific structure that will be described in detail is an area called vasotubulus area here. Some vascular strands in nodes are so different from the usual collateral internode bundles and they are so prominent that they are defined as vasotubuli in this paper. In fully developed nodes of *Avena* species, they can be detected with the naked eye. They cannot just be described as 'thick bundles' as we will see.

Before all levels are described in detail, it makes sense to follow the longitudinal course of selected bundles through a node first. In Fig. 4, A we can see a single bundle entering the node from below and becoming thicker in the nodal area. The thicker part is the vasotubulus. The depicted example is not fully developed yet being thinner than those at older nodes. What we can see in Fig. 4, A is a typical leaf trace that leaves the stem at the node. In Fig. 4, B both leaf traces and axial or cauline bundles are stained. What we recognize is that the axial bundles seem to hit a vasotubulus from above and split. A few transverse bundles are stained in the centre of the node. These bundles are part of the so called nodal plexus.

In Fig. 5, single bundles are stained in the apical region of wheat and oats. It becomes clear that some bundles leave as leaf traces at node N (N2 in the case of the wheat example and N3 in the oats example). Others, the axial bundles, pass by. They run through the upper internode before they leave at node N-1 (N1 in the wheat figure and N2 in the oats figure).

Fig. 6 shows what happens where axial bundles meet vasotubuli in fully developed nodes. The bundles split at level D as described in Fig. 4, sometimes in two separate bundles as seen in the left part (*Echinochloa crus-galli*). This is, however, not always the case. Sometimes, many loop forming, small bundles arise which merge again below the vasotubulus as shown for *Dactylis glomerata* and *Avena sativa*. At the lower end of the node, vasotubuli change their shape and end in collateral bundles again (level A).

Now, it is time to describe the bundle modifications as seen in transverse sections. The changes are explained from the bottom to the top. Level A is at the basal end of the node.

Level A – Lower nodal transition zone (LNTZ). At the border between internode and node, the anatomy of the vascular bundles starts to change in all investigated species. Cells in the xylem area of some bundles start to divide and to differentiate into new vascular elements (Fig. 7). Especially metaxylem elements are augmented as can be seen in the bundle of *Festuca gigantea* at the bottom of Fig. 7 (A). Longitudinal sections show that vascular bundles increase in diameter as we can see in the picture of *Dactylis glomerata* to the right.

Level B – Lower vasotubulus zone (LVZ). The phloem part of the original bundles becomes completely surrounded by metaxylem elements at level B (Fig. 7, B). Protoxylem elements stay attached.

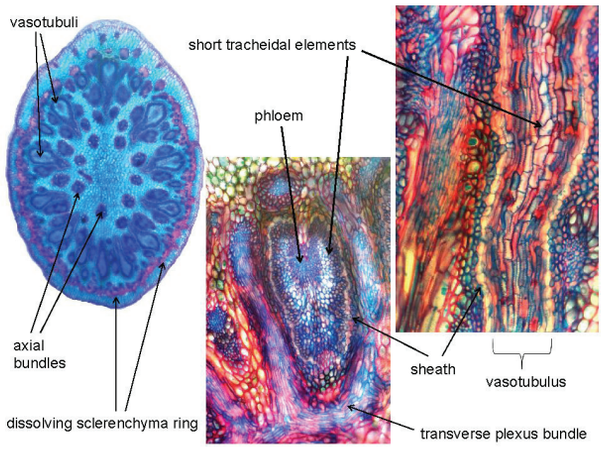

Fig. 8. Zone C of grass nodes. Left: *Setaria glauca* transverse, overview; central axial bundles are surrounded by pear-shaped vasotubuli, Etzold blue, ~20×**; m**iddle: *Avena sativa* transverse; central vasotubulus is surrounded by transversally running nodal plexus element, Etzold blue, ~100×**; right:** *Avena sativa* longitudinal, vasotubulus with short tracheidal elements is surrounded by a distinct sheath; Etzold blue, 400×

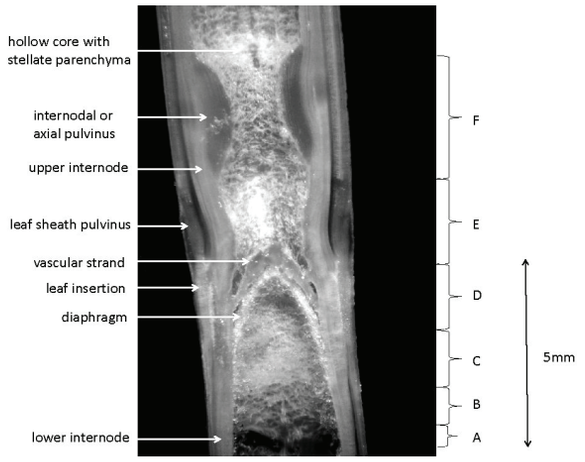

Fig. 9. A macro view of longitudinally cut *Phragmites australis* culm at node

The original bundle becomes surrounded by a new, 1–2-layered sheath.

Level C – Upper vasotubulus zone (UVZ). The modified bundles or strands become primarily heart-, pear- or droplet shaped in transverse sections. These bundle-like strands are called vasotubuli here as explained before. Longitudinal sections make clear that the xylem and phloem elements are running primarily in vertical direction within vasotubuli. Fig. 8 shows how vasotubuli are arranged in a ring-like form in *S. glauca.* Not all vascular bundles are converted into vasotubuli. Some bundles in the inner area stay rather unmodified or are only slightly changed. Those are axial bundles which do not leave the stem but continue their course into upper internodes.

Level D – Leaf insertion zone (LIZ). At level D, peripheral sclerenchymatic rings dissolve in the pulvinus area. Some bundles find their way into the attached leaf, others continue into the following internode. Several bundles turn horizontally and become part of the nodal plexus. These plexus elements are amphivasal bundles. They surround vertical bundles and form transverse connections with the bundle system of the newly formed internode.

Level E – Funnel or pulvinus zone (FZ). Finally, vasotubuli bend outwards into the attached leaf consisting of the pulvinus at this level (Fig. 3). Small bundles are part of the nodal plexus and surround the outward bending strands, they also form the connection of sclerenchymatic rings in subsequent phytomers. In the funnel area, many bundles are at a very early developmental stage with all initial protoxylem elements still apparent. A protoxylem cavity is not visible in most bundles. The peripheral bundles are embedded in a tissue of small diameter and thin walled cells.

Level F – Internode separation zone (ISZ). Pulvinus and the new internode are not separated at the base of the new internode. A few millimetres above, leaf sheath, internode with a bud groove and buds appear in many species and the upper internode separates from the leaf sheath.

Modifications of the vascular system at different levels of *Phragmites australis*

Fig. 9 shows an overview of a longitudinally cut *P. australis* node equivalent to the pooid node in Fig. 3. The nodal zones are however somewhat different insofar as *P. australis* forms an internodal or axial pulvinus in addition to the leaf sheath pulvinus. Transverse bundles can be found directly above the diaphragm in the nodal zone. Stellate cells partially fill the hollow stem core within the nodal area.

The internode anatomy of *P. australis* does not look very specific compared with other grass species: collateral bundles are arranged in ring-like forms around a hollow core (Fig. 10, top left). The changes detectable in different nodal zones are described below.

Level A – Lower nodal transition zone (LNTZ). At the lower border to the node, the anatomy of the larger, central vascular bundles starts to change (Fig. 10, A). Phloem and xylem elements are augmented.

Level B – Lower vasotubulus zone (LVZ). Phloem and xylem parts start to split (Fig. 10, B).

Level C – Upper vasotubulus zone (UVZ). Three distinct bundles connected with the original internode bundle become visible in *P. australis*, the developing vasotubulus in the centre and two accompanying 'regular' bundles (Fig. 10, C).

Level D – Leaf insertion zone (LIZ). Some phloem parts of strands adjacent to the central vasotubulus undergo major changes. Phloem elements become narrow. A differentiation between sieve tubes and companion

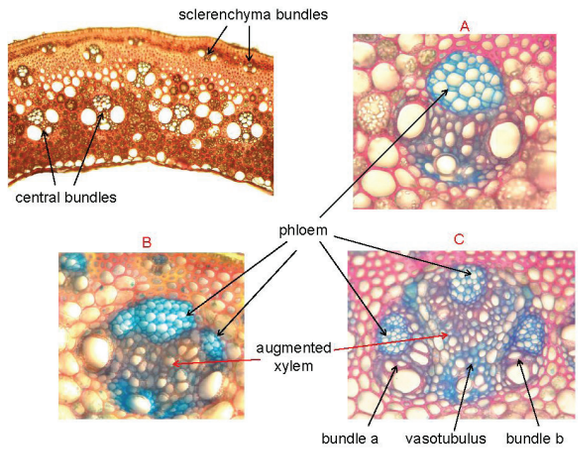

Fig. 10. *Phragmites australis*, transverse sections of internode (top left) and three different nodal zones: level A (top right), level B (bottom left), level C (bottom right)

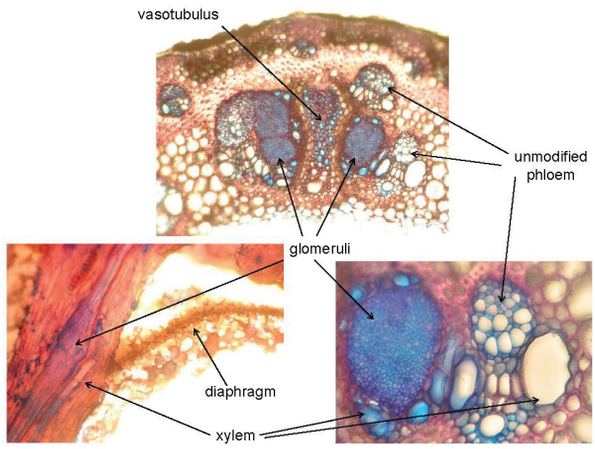

Fig. 11. Top: nodes of *Phragmites australis* with glomeruli; transverse section at level D (top) and enlarged right, longitudinal section bottom left

cells is no longer possible at a light microscope level (Fig. 11). Such structures are called glomeruli here. They are primarily located in the diaphragm area as shown in the longitudinal section (Fig. 11, bottom left). Finally, round strand complexes are formed by *P. australis* (Fig. 12, A) which consist of a central vasotubulus directly surrounded by several slightly modified bundles or strands. Characteristic of the complexes in *P. australis* is a protecting sclerenchymatic outer casing.

Level E – Funnel or pulvinus zone (FZ). The strand complexes get separated and slightly modified again. Single sclerenchyma bundles located between the complexes turn into the leaf base and become intermediate size bundles (Fig. 12, B). Vasotubuli turn into leaves and form major bundles.

DISCUSSION

The ring-like structures, characteristic elements in internodes, are a result of the arrangement of leaves along culms. Leaf sheaths surround the stem. Bundles entering the node from sheaths below the pulvinus are therefore arranged in a ring-like form in many species. Prominent, mostly enlarged bundles are descendants of the median strand as already described by A r b e r (1934). Due to the distich arrangements, we usually find two median descendants opposite to each other. Some bundles run through several nodes before they leave the stem and turn into leaves. This is why the number of bundles entering at a given node is different from the number of vascular bundles in the internode below. The fate of the peripheral sclerenchyma bundles has not been clear so far. Some papers regard them as branches of stem bundles, others as descendants of small leaf bundles (P a t r i c k , 1972a). Apparently, some sclerenchyma bundles continue, however, from one internode into the next one. Others become part of the nodal plexus and some enter the leaf attached to the node.

The fact that many bundles change their shape within nodes makes an analysis of their course difficult. Several authors such as H i t c h , S h a r m a n (1971) were aware of bundle modifications in grass nodes. This is why they often use the term strand instead of bundles. Y a m a j i , M a (2014) talk of enlarged vascular bundles (EVB), transit vascular bundles (TVB), and diffuse vascular bundles (DVB). The enlarged bundles or EVBs are actually identical with leaf traces, with obstructing strands (H i t c h ,

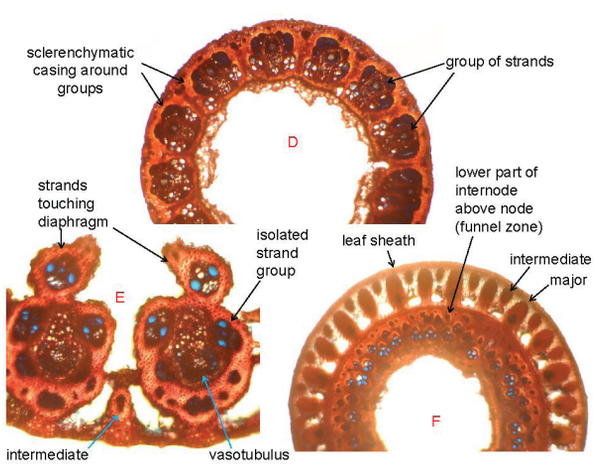

Fig. 12. Transverse sections of *Phragmites australis* nodes at levels E and F. Top: encased strand groups with glomeruli at the border between levels D and E; bottom left: separating strand complexes near diaphragm, glomeruli turn into bundles, single bundles between strand groups form framework for leaf, central vasotubuli start turning into leaf base; bottom right: newly forming upper internode surrounded by leaf sheath in zone F, major leaf bundles are connected with vasotubuli

S h a r m a n , 1971) or elliptical bundles (O ' B r i e n , Z e e , 1971). These strands are called vasotubuli here as they do not have much in common with vascular bundles any more.

S h a n e et al. (2000) report on 'irregular connecting xylem elements' in the nodes of *Z. mays,* which are presumably identical with the elements in vasotubuli. Vasotubuli may be defined as amphivasal. They differ, however, considerably from classic amphivasal bundles as we find them e.g. in *Acorus* species (K r a e h m e r , 2016). Axial bundles or bypassing bundles split where they meet vasotubuli. In many cases they split into two halves as depicted in some articles. They may, however, also split into several branches. These axial bundles are called obstructed bundles e.g. by H i t c h , S h a r m a n (1971). Most sketches of these bundles make the impression as if the obstructed bundles merge with the obstructing bundles. This is, however, definitely not the case. The single elements may form loops around the vasotubuli as shown in Fig. 6. Other axial bundles, primarily the most inner ones, run almost unchanged through the stem. They are called alternating strands by H i t c h , S h a r m a n (1971) and may be called axial or cauline from time to time.

The high number of small plexus bundles in many nodes show that vascular strands can be intensively connected. These connections guarantee an optimum distribution of water and solutes including minerals and sometimes xenobiotics such as fungicides, insecticides or herbicides in culms of grasses.

The nodes of *Phragmites australis* are very peculiar. The bundles are grouped within nodes into complexes. This phenomenon has been observed in *Arundo donax* also in part (not reported here). A very special item found in *Phragmites* nodes are glomeruli as they exist in nodes of the Dioscoreaceae family (A y e n s u , 1972) and in the Poaceae subfamily Bambusoideae (L i e s e , 1998). Gene sequencing technologies should make it possible to demonstrate which gene sequences these representatives have in common.

Unfortunately, the three-dimensional structure of grass nodes is quite complicated. This is why the description of nodal elements in grasses has been neglected to some extent in the recent past. This situation seems to change now as molecular biologists (e.g. G e e t a , 2016) try to find specific genes (such as KNOX genes) which seem to play a central role in the arrangement of vascular bundles in angiosperms. Also, new three-dimensional analysis technologies such as X-ray μCT imaging technique will improve the direct demonstration of bundles courses (P e n g et al., 2014).

CONCLUSION

Many representatives of the Poaceae family are either crops or weeds. The distribution of agrochemicals in vascular bundles has been an interesting topic for studying the development of new molecules in the past. Most registration studies are based on radiolabelled compounds and do not consider structural specific structures in nodes which should explain why compounds are transported there. Recent literature data indicate that the distribution of assimilates, nutrients, and solutes is redirected in grass nodes. This makes gene expression in nodes a potential tool for influencing yields. Grass nodes are different from those of other monocot species. Their three-dimensional structure is complicated and many phenomena are still unexplained. This paper provides a basis for more detailed investigations of processes that explain the distribution of solutes within grasses. It describes new structures such as glomeruli in *Phragmites australis* and contributes therefore to the understanding of evolutionary developments in grasses.

REFERENCES

Arber A (1934): The Gramineae. Cambridge University Press (reprint 2010), Cambridge.

Ayensu ES (1972): Anatomy of the monocotyledons. VI. Dioscoreales. Clarendon Press, Oxford.

Bell AD (1976a): The vascular pattern of Italian ryegrass (*Lolium multiflorum* Lam.) 2. Development of the seedling axis to maturity. Annals of Botany, 40, 233–240.

Bell AD (1976b): The vascular pattern of Italian ryegrass (*Lolium multiflorum* Lam.) 3. The leaf trace system, and tiller insertion, in the adult. Annals of Botany, 40, 241–250.

Bell AD, Wynn Parry D (1976): The vascular pattern of Italian ryegrass (*Lolium multiflorum* Lam.) 1. The young seedling and its variability. Annals of Botany, 40, 223–232.

DeMason DA (1994): Stem thickening in monocotyledons. In: Iqbal M (ed.): Growth patterns in vascular plants. Dioscorides Press, Portland, 288–310.

Esau K (1943): Ontogeny of the vascular bundle in *Zea mays.* Hilgardia, 15, 327–368.

Fahn A (1990): Plant anatomy. Pergamon Press, New York.

Forster BP, Franckowiak JD, Lundqvist U, Lyon J, Pitkethly I, Thomas WTB (2007): The barley phytomer. Annals of Botany, 100, 725–733.

Fournier C, Andrieu B (2000): Dynamics of the elongation of internodes in maize (*Zea mays* L.): analysis of phases of elongation and their relationships to phytomer development. Annals of Botany, 86, 551–563.

Geeta R (2016): KNOX genes and shoot development in angiosperms: old actors in new roles? Phytomorphology, 66, 57–69.

Henkel K (2003): Die Mikrofibel. Mikrobiologische Vereinigung München e.V. http://www.klaus-henkel.de/mikrofibel.pdf. Accessed 26 June, 2016. (in German)

Hitch PA, Sharman BC (1971): The vascular pattern of festucoid grass axes with particular reference to nodal plexi. Botanical Gazette, 132, 38–56.

Hoshikawa K (1989): The growing rice plant – an anatomical monograph. Nobunkyo, Tokyo.

Kraehmer H (2016): Atlas of weed mapping. Wiley-Blackwell, Chichester.

Kraehmer H, Baur P (2013): Weed anatomy. Wiley-Blackwell, Oxford.

Kumazawa M (1942): The origin and structure of the nodal plexus of *Zea mays*. I. Vascular anatomy in maize. IV. The Botanical Magazine Tokyo, 56, 528–536.

Kumazawa M (1946): Vascular anatomy in maize. V. The developmental order of the vascular system, together with the course of compound and outermost peripheral bundles in the system of *Zea mays*. The Botanical Magazine Tokyo, 59, 42–52.

Kumazawa M (1961): Studies on the vascular course in maize plant. Phytomorphology, 11, 128–139.

Lersten NR (1987): Morphology and anatomy of the wheat plant. In: Heyne EG (ed.): Wheat and wheat improvement. American Society of Agronomy, Madison, 33–113.

Liese W (1998): The anatomy of bamboo culms. International Network for Bamboo and Rattan (INBAR), Technical report No. 18, Beijing.

O'Brien TP, Zee S-Y (1971): Vascular transfer cells in the vegetative nodes of wheat. Australian Journal of Biological Sciences, 24, 207–217.

Patrick JW (1972a): Vascular system of the stem of the wheat plant. I. Mature state. Australian Journal of Botany, 20, 49–63.

Patrick JW (1972b): Vascular system of the stem of the wheat plant. II. Development. Australian Journal of Botany, 20, 65–78.

Peng G, Jiang Z, Liu X, Fei B, Yang S, Qin D, Ren H, Yu Y, Xie H (2014): Detection of complex vascular system in bamboo node by X-ray μCT imaging technique. Holzforschung, 68, 223–227.

Pizzolato TD (2000): A systematic view of the development of vascular systems in culms and inflorescences of grasses. In: Jacobs SWL, Everett J (eds): Grasses: systematics and evolution. CSIRO Publishing, Collingwood, 8–28.

Shane MW, McCully ME, Canny MJ (2000): The vascular system of maize stems revisited: implications for water transport and xylem safety. Annals of Botany, 86, 245–258.

Sharman BC (1942): Developmental anatomy of the shoot of *Zea mays* L. Annals of Botany, 6, 245–284.

Stover EL (1934): Development and differentiation of tissues in the stem tips of grasses. Ohio Journal of Science, 24, 150–160.

Tomlinson PB (1995): Non-homology of vascular organisation in monocotyledons and dicotyledons. In: Rudall PJ, Cribb PJ, Cutler DF, Humphries CJ (eds): Monocotyledons: systematics and evolution. Royal Botanic Gardens, Kew, 589–622.

Wacker R (2006): Eine neue und einfache Methode zur polychromatischen Anfärbung von Paraffinschnitten pflanzlicher Gewebe für Durchlicht- und Fluoreszenzmikroskopie. Mikrokosmos, 4, 210–212.

Yamaji N, Ma JF (2009): A transporter at the node responsible for intervascular transfer of silicon in rice. Plant Cell, 21, 2878–2883.

Yamaji N, Ma JF (2014): The node, a hub for mineral nutrient distribution in graminaceous plants. Trends in Plant Science, 19, 556–563.

Zimmermann MH, Tomlinson PB (1972): The vascular system of monocotyledonous stems. Botanical Gazette, 133, 141–155.

Corresponding Author:

Dr. Hansjoerg K r a e h m e r, Kantstrasse 20, D-65719 Hofheim, Germany, phone +49 6192 296560,
e-mail: Kraehmer-Hofheim@t-online.de